Impact of the plutonium content on dissolution kinetics of $(U_{1-x}Pu_x)O_{2\pm\delta}$ powders

Yannis Ziouane, Bénédicte Arab-Chapelet, Gilles Leturcq

Impact of the plutonium content on dissolution kinetics of $(U_{1-x}Pu_x)O_{2\pm\delta}$ powders

Yannis ZIOUANE [a], Bénédicte ARAB-CHAPELET [b], Gilles LETURCQ [b]

[a] ORANO Projets – Research Hall of Beaumont-Hague, 30440 Beaumont-Hague
[b] CEA, DES, ISEC, DMRC, University of Montpellier, Marcoule, France

Corresponding author:
E-mail address: gilles.leturcq@cea.fr (G.LETURCQ)
Full postal address: CEA Marcoule, bât 57. 30207 Bagnols-sur-Cèze Cédex

Keywords

UO_2, PuO_2, mixed oxides, syntheses, characterization, dissolution kinetics, plutonium content, powder.

Abstract

Several $(U_{1-x}Pu_x)O_{2\pm\delta}$ powders with different morphologies and different plutonium contents were synthetized using a sol-gel route. All the powders were fully characterized to quantify their structural parameters. After understanding and verification of the morphological effects on mixed oxide dissolution, this study consists of quantification of effect of plutonium content on dissolution kinetics using nitric acid 8.5M at 95°C. Significant differences in dissolution kinetics were observed. Indeed, the plutonium content is a key parameter that has to be considered in studies of $(U_{1-x}Pu_x)O_{2\pm\delta}$ dissolution kinetics. A kinetics law was established and validated for dissolutions within these particular experimental conditions.

1. Introduction

The dissolution of spent nuclear fuel in nitric acid is one of the main steps of nuclear fuel recycling by hydrometallurgical process. For this purpose, it is useful to fully understand and quantify the impact of fuel characteristics on dissolution kinetics. In this study, a focus on the impact of the plutonium content of the (U,Pu) oxide on dissolution kinetics was done. Only a few studies were focused on this effect, because of the high radioactivity of these materials and the difficulties to manipulate plutonium.
Uriarte *et al.* [1] presented the differences in dissolution kinetics between UO_2 and PuO_2 in nitric medium. The authors described that dissolution kinetics, using nitric acid at 5 $mol.L^{-1}$, are approximately twenty million times faster for UO_2 compared to PuO_2. For the mixed oxide, they found that the more the mixed oxide contains plutonium the slower the dissolution kinetics. Lerch [2] also described a strong impact of the plutonium content on the kinetics and solubility of the oxides. The author studied oxides with Pu contents ranging from 15 to 25 percent. In this interval, the author proposed to model the impact of Pu amount on dissolution kinetics with a linear regression. Ikeuchi [3] studied the impact of Pu content ranging from 18 to 29% on spent fuel. Irradiated MOX (Mixed OXides) with Pu content of 18% was estimated to be similar to irradiated fuel LWR (Light-Water Reactor) of FBR axial blancket fuel in term of solubility, although it contains less plutonium in composition,. Above a plutonium content of 18%, the author indicated an exponential decrease of the

dissolution kinetic rate with a linear increase of Pu content, and provided an empirical law also taking into account the acidity and temperature. Vollath [4] studied the (U,Pu) oxide dissolution at different Pu content, ranging from 0 to 100%, varying the acidity for a time period of 6 hours. The author observed no residue at the end of the dissolution of $(U_{1-x}Pu_x)O_{2\pm\Delta}$ mixed oxide with a plutonium content up to 40%. Beyond this value, the percentage of residues increases exponentially until reaching about 100% when the Pu content is greater than 70%.
All these authors did not consider the effect of the morphology of the material on dissolution kinetics. Indeed, for UO_2 [5] and PuO_2 [1,6] there are differences in dissolution kinetics which can vary by a factor of twenty depending on the morphology of the materials. Thus, no valid law has yet been determined describing the effect of the Pu content on dissolution kinetics. In 1967, studying the dissolution of non-irradiated PuO_2 in hydrochloric acid and in nitric acid-calcium fluoride solvent system, Molen [7] described the effect of the solid-to-liquid ratio on the dissolution rate of plutonium oxide as a function of the morphology, and more particularly the mean crystallite size and the specific surface area, which in turn depends on porosity, pore size distribution, shape, size, and roughness. Among these two parameters, the author indicated that the specific surface area is the predominant parameter. Recently [8], the effect of morphology of the oxide on the dissolution rates has been quantified on CeO_2 and validated on PuO_2, evaluating the impact of each morphological parameter could have on the dissolution rates in nitric medium, over a wide range of morphological parameters. Statistically significant effects of crystallite sizes and specific surface area on the dissolution rates were formulated, in the same way Molen had presented. In addition, an empirical law describing how these parameters impact the dissolution kinetics rates was established. All these studies have in common the comparison of compounds with the same "initial mass of oxide/ initial volume of solution" ratio. For a given amount of solid, dissolution kinetic rate increases with higher specific surface area or lower crystallite size owing to more contact between solid particles and solution.
In the first part of this work, a study using different morphologies at the same Pu content has been conducted to validate this morphological law on the dissolution rates whatever the Pu content. In a last part, tests on mixed oxides permit to define an empirical model describing perfectly the effect of the Pu content on the dissolution rates taking care of the morphology of the samples. This paper presents our contribution done recently in Atalante facility at CEA Marcoule to understand the phenomena occurring during the dissolution of actinide oxides in nitric acid.

2. Experimental section

2.1. Synthesis of $(U_{1-x}Pu_x)O_{2\pm\delta}$ powders

2.1.1. Sol-gel route

Synthesis of (U,Pu) oxides using sol-gel route require the use of low acidic and highly concentrated cationic solutions. A 2.9 M U(+VI) monometallic acid deficient uranyl nitrate (ADUN) solution was obtained in a glove-box under negative pressure through dissolution of uranium trioxide into uranyl nitrate solution till solubility limit was reached. After two weeks of stirring, the UO_3 excess was filtered from the ADUN solution. The free acidity of the ADUN solution was very low as its pH was around 1.8.

In parallel, a 2.14 M Pu (+IV) monometallic nitrate solution was prepared by concentration/denitration process of a 0.24 M Pu(+IV) monometallic nitrate solution. In order to concentrate a Pu nitrate solution without concentrating the free nitric acidity, a distillation column was used with frequent additions of nitric acid solution of low acidity. Ideally, water should be used but the addition of water would cause Pu hydrolysis locally prior to the mixing of the solution. As shown in Figure 1, the more acidic the solution to be evaporated, the more acidic the vapor and the effective denitration [9]. Therefore, it is better to add small amount of low acidic solution frequently than larger

amount less often, to keep the acidity of the solution to distillate as high as possible during the process of denitration.

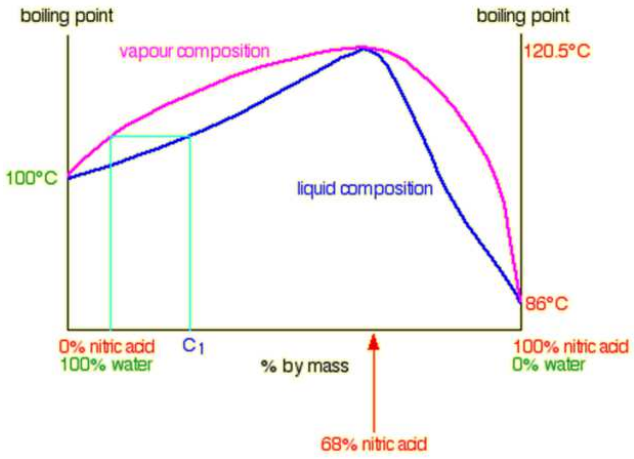

Figure 1 : Distillation of nitric acid, link between acidity of the solution to be evaporated and the acidity of the vapor produced.

Addition of nitric acid solution of concentration below 0.5M causes Pu hydroxide colloids generation. Nitric acid of 0.5M was therefore used. As described in Figure 1, the acidity of the solution to evaporate has to be higher than 3M in order to evaporate more nitric acid than the 0.5M added. Using this method, a Pu solution with [Pu] =510g.L^{-1} and [HNO_3] = 1.85 M was obtained.

Articles referring to the sol-gel method deal with the synthesis of microspheres [10,11]. In this paper, protocols were modified to synthesize powders as follows. For the different mixed oxides to produce, corresponding volumes of both solutions were then mixed with the desired stoichiometric ratio for the final oxide. Urea $CO(NH_2)_2$ and HMTA (hexamethylenetetramine) solution at low temperature (~5°C) were added to this mixed metal solution. The ratio [HMTA]/[U+Pu] used was equal to 2.0 [12] while [urea]/ [U+Pu] was 1.7. Once HMTA was dissolved into the cold nitrate solution, the solution was stirred and heated at 80°C. HMTA decomposed at high temperature causing an increase in pH and simultaneous hydrolysis of U and Pu. In a few minutes, solution turned to a gel. For a gel with a [Pu]/[U+Pu] ratio equal to 61% the ratios of the reagents were increased by 20% in order to change the pH of the gelation and therefore attempted to modify the morphology parameters of the final oxide to compare with a "61%" oxide made using the standard ratios. At room temperature, gel were washed with 2 M NH_4OH allowing the elimination of the remaining organic matter provided by the reagents. The washed gels were calcined at 220°C for 30 min to remove residual ammonium nitrate and moisture. The dried gels were then calcined under reduced atmosphere Ar/H_2 (95/5) to form the different oxides.

2.1.2. Thermal treatments

Heat treatments were performed up to 850°C with a rate of 20°C.min^{-1} for a majority of the gel. Compounds were maintained to this temperature for 90 min then cooled down to room temperature. A reducing atmosphere Ar/H_2 (95/5) was used for these calcinations in order to reduce the uranium to its lower valence (+IV) and therefore have a solid solution $(U_{1-x}Pu_x)O_{2\pm\delta}$. These conditions are identical to those used by Ziouane et al. [5] for the UO_2 synthesis. This study confirmed the complete reduction of U(+6) to U(+4). To have more than two morphologies with the same Pu content (i.e. 61%), a gel after its synthesis was separated into two batches: the first batch was calcined at 850°C and the other at 1000°C. It has already been shown [13,14] that the increase of the calcination temperature contributes to the densification of the material by decreasing the specific surface area and increasing the crystallite sizes. The powder containing 36% of plutonium was obtained after three calcination cycles including one at 1500°C. At this Pu content, the powder is highly reactive with

respect to dissolution[4], all these cycles of calcination were carried out in order to make the powder more refractive to dissolution.

2.2. Characterization

2.2.1. XRD Analysis

XRD (X-Ray Diffraction) analyses of the synthesized powders were performed using a D8 Bruker Advance diffractometer (LynxEye detector) using Cu-Kα radiation (λ=1.5418 Å) especially equipped for radioactive material measurements. Gold was added as an internal standard to calibrate the angular positions of the observed XRD lines. Each powder pattern was recorded within an angular range from 5° to 80° in 2theta, with steps of 0.02° and a counting time of 0.6 s per step. The lattice parameters were determined by Le Bail refinement using the TOPAS software (TOtal Pattern Analysis Solutions) from BRUKER AXS [15] where only the profile parameters (cell dimensions, peak shapes, background, zero point correction) were refined. The microstrains and average crystallite sizes were calculated with the fundamental parameters method [16].

2.2.2. Specific surface area measurements

N_2 adsorption/desorption isotherm was used for the determination of the biggest specific surface area (> 1 $m^2.g^{-1}$) and the pore volume, Kr adsorption/desportion was used for smaller specific surface area. The specific surface area was calculated by the Brumauer-Emmett-Teller (BET) 5 point method [17] from around 1 g of each powder. Adsorption – desorption isotherms were measured at the boiling point of nitrogen (-196 °C) using a Micromeritics TriStar II Version 1.03 nuclearized.

2.2.3. Analysis of uranium and plutonium concentrations in solution by TIMS (Thermal Ionization Mass Spectrometry)

To determine precisely the $\frac{[Pu]}{[U+Pu]}$ stoichiometry of the synthesized oxides, a complete dissolution of the material was carried out in boiling HNO_3/HF (4 M/0.05M) medium. A sample was taken when the powder was completely solubilized, the total dissolution liquor left over was then recycled to recover uranium and plutonium for further experiments using a partitioning column as described by Maillard et al. [18].
An isotopic analysis was then performed by thermo-ionization to produce ion beams in the TIMS mass spectrometer. The spectrometer used is a Thermo Fisher Scientific Triton. The method involves the evaporation and ionization by heating a dilute solution to be analyzed deposited on a metal ribbon using a micro syringe. The solution is then dried and installed in the source of the instrument. The ribbon is then heated by vacuum Joule effect, allowing the evaporation and ionization of the sample, to form an ion beam which is then analyzed in the mass spectrometer. Ion collectors detect the different beams produced by mass separation. The results are presented as isotopic ratios, given by the measured relative intensities of the different beams.

2.3. Dissolution

All the dissolutions described in this work were carried out in a glove box under negative pressure (Figure 2) and consisted of dissolving 300 mg of $(U_{1-x}Pu_x)O_{2\pm\delta}$ powder in 15 mL of nitric acid of 8.5 $mol.L^{-1}$ concentration. Solution was stirred at 300 rpm and maintained at 368.15 K. 2 h batch dissolutions were performed in a 60 mL maximum capacity reactor. These aggressive conditions are

selected because of the refractory character of the oxides to dissolution in nitric medium. The lid of the reactor was equipped with a refrigerating column allowing the recombination of any nitrous vapors escaping from the reactor. The aim of these dissolution experiments was to understand how the Pu content impact dissolution kinetics. The different dissolution kinetics rates were recorded by alpha counting. This device allows determining the plutonium concentration in solution, the uncertainties applied to the experimental measurement are equal to 10% from pre-established standards. The congruence of uranium and plutonium has been verified and the mixed powders dissolve homogeneously. Considering their radioactivity all the liquid effluents of this study were recycled to recover Pu and U for a future study, using separation columns such those used by Maillard et al. [18].

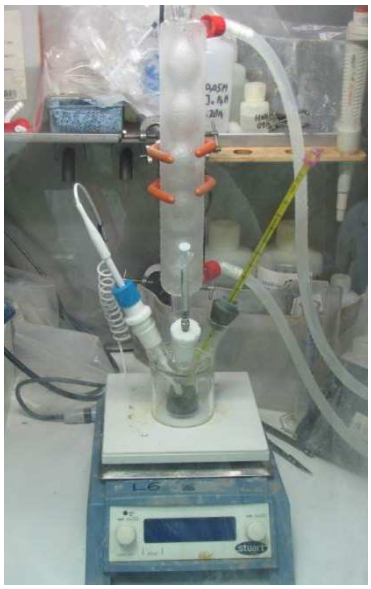

Figure 2 : Photograph of a dissolution test with the stirred and heated solution in a glove-box under depression. The four nozzles on the reactor are used for the temperature regulation and control, the sampling of the solution and the refrigerating column.

3. Results and discussion on $(U_{1-x}Pu_x)O_{2\pm\delta}$ samples

3.1. Structure and morphology characterizations

Structural description

The Pu stoichiometry of the different samples determined by TIMS are reported on Table 1. For all powder samples, XRD patterns were characteristic of a fluorite-type $(U_{1-x}Pu_x)O_{2\pm\delta}$ structure. Within the XRD detection limits, there was thus no additional phase. Table 1 also gathers the structural parameters of the different oxides. The lattice parameters vary with the Pu content according to the Vegard's law (3.1.1). This law was plotted in Figure 3 from the values presented by Young *et al.* [19] for UO_2 and Freeman *et al.* [20] for PuO_2. The experimental lattice parameters are nearly perfectly aligned with this law, indicating that they correspond to the theoretical lattice parameters calculated from the TIMS characterization. In the case of $U_{0.39}Pu_{0.61}O_{2\pm\delta}$ (Expt. No. 850 a), there is a slight deviation from the line corresponding to a slight sub-stoichiometry of the compound, as shown in Table 1.

$$a_{theoretical} = -0.071 * \frac{[Pu]}{[U+Pu]} + 5.467 \qquad 3.1.1$$

This deviation from Vegard's law can be explained by variation in oxygen. From the experimental lattice parameter, it is possible to calculate the oxygen stoichiometry of the oxide $(U_{1-x}Pu_x)O_{2\pm\delta}$ from the empiric law (3.1.2) [21].The fourth column of the table 1 shows the results of this calculation for each material, leading to a perfect stoichiometry, with the uncertainty, for each compound.

$$\delta = \frac{5.467 * (1 - x) + 5.396x - a_{experimental}}{0.112} \qquad 3.1.2$$

The oxides resulting from the same calcination temperature presents similar average crystallite sizes (Table 1). Furthermore, the average crystallite sizes seem to increase with the precursors calcination temperature, in accordance with data from the literature describing crystal growth during the sintering process [14].

The specific surfaces obtained are all of the same order of magnitude and small, but are also in accordance with the values already obtained in the literature for actinide oxides[22].It also appears from the table that the specific surface area of the oxides appear to be lower when the calcination temperature applied to obtain the oxide was higher.

Table 1 : Structural parameters for each powders of $(U_{1-x}Pu_x)O_{2\pm\delta}$ synthetized by sol-gel route and calcined at different temperature.

Compound	Calcination temperature (°C)	Lattice parameter (Ă)	O/ (U+Pu)	Average crystallites sizes (nm)	Specific surface area ($m^2.g^{-1}$)
$U_{0.64}Pu_{0.36}O_{2\pm\delta}$	1500	5.4419 (1)	2.01 (2)	48 (1)	0.4 ± 0.3
$U_{0.43}Pu_{0.57}O_{2\pm\delta}$	850	5.4276 (1)	1.99 (2)	49 (1)	0.4 ± 0.3
$U_{0.39}Pu_{0.61}O_{2\pm\delta}$	850 a	5.4321 (1)	1.92 (2)	43 (1)	1 ± 0.1
	850 b	5.4228 (1)	2.01 (2)	33 (1)	1.5 ± 0.3
	1000 c	5.4241 (1)	2.00 (2)	69 (2)	0.9 ± 0.2
$U_{0.24}Pu_{0.76}O_{2\pm\delta}$	850	5.4131 (1)	2.04 (2)	56 (2)	2.2 ± 0.2
PuO_2	850	5.3980 (1)	1.98 (2)	17 (1)	6.3 ± 0.5

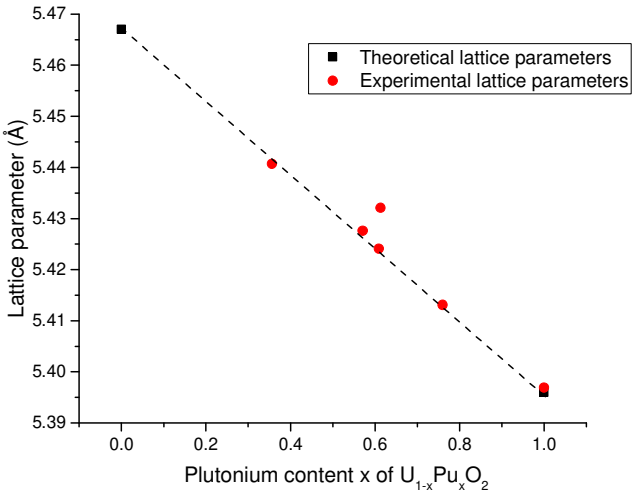

Figure 3: Evolution of the lattice parameter with Pu content in $(U_{1-x}Pu_x)O_{2\pm\delta}$ solid solution, measured by XRD and compared with Vegard's law of $(U_{1-x}Pu_x)O_2$.

3.2. Validation of the morphologic law

Ziouane *et al.* [8] presented the impact of powder morphology on dissolution kinetics of CeO_2 and PuO_2 defining an empirical law based only on the crystallite size and the specific surface area of the powder. To perfectly describe the effect of the Pu content, it is essential to validate that the effect of the morphology induced on dissolution is valid for $(U_{1-x}Pu_x)O_{2\pm\delta}$. Thus, three $U_{0.39}Pu_{0.61}O_{2\pm\delta}$ were synthesized with different crystallite sizes and surface areas (Table 1). These oxides were dissolved under the same experimental conditions and the kinetics rates of dissolution are shown in Figure 4. The figure shows that at the same Pu content, the dissolution rate can vary by a factor of 4 only due to morphological differences. This report is not surprising because Ziouane *et al*. also observed the same behavior on CeO_2 compounds: dissolution rate can vary by a factor close to twenty for CeO_2 powders presenting different morphologies.

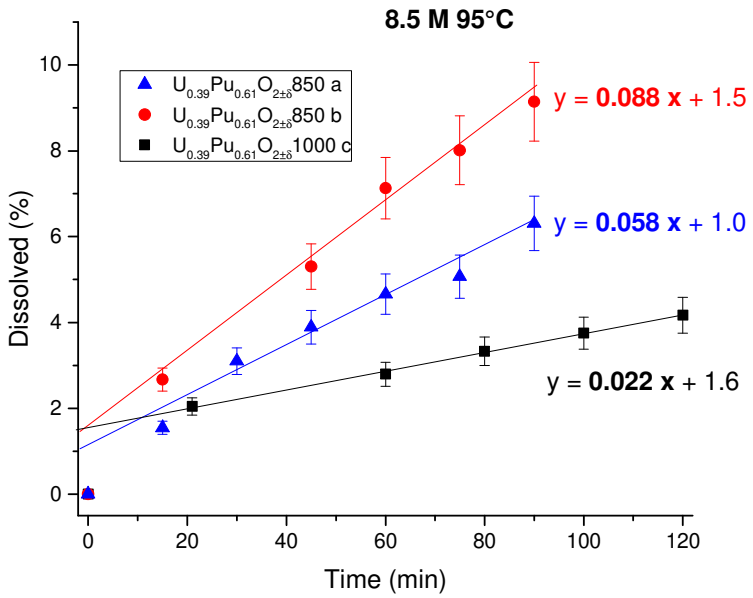

Figure 4 : Dissolution of three$U_{0.39}Pu_{0.61}O_{2\pm\delta}$ powders in concentrated nitric medium 8.5 mol.L^{-1} for a dissolution temperature of the system equal to 95°C.

The partial orders for the crystallite sizes and the specific surface area determined previously by the kinetic laws of CeO_2 and PuO_2 [1] are retained, -1 and 1/3 respectively. The resolution of the system of three equations with an unknown leads to the empirical law 3.2.1. A specific k value was found for $U_{0.39}Pu_{0.61}O_{2\pm\delta}$ powders, independent of the powder morphology. This value expresses the possibility to describe satisfactorily the kinetics of dissolution from the morphological characteristics of the powders. Hence, this empiric morphologic law being verified for CeO_2, PuO_2 and here $U_{0.39}Pu_{0.61}O_{2\pm\delta}$, it applied to all uranium, plutonium mixed oxides making possible to dissociate, under same experimental conditions, the effects of the Pu content and the morphological effects.

$$y = k * Tc^{-1} * SSA^{0.33} \qquad 3.2.1$$

With y the dissolution kinetic rate in %dissolved.min^{-1}, k = $10^{0.35}$ nm^{-1}.m$^{-2/3}$.g$^{1/3}$.%dissolved^{1}.min^{-1} for $U_{0.39}Pu_{0.61}O_2$ being dissolved in nitric acid 8.5M at 95°C, Tc the crystallite size in nm, SSA the specific surface area in m^2.g^{-1}.

3.3. Dissolution kinetics of $(U_{1-x}Pu_x)O_{2\pm\delta}$ materials

The experimental conditions of dissolution of all samples of this study were kept constant (i.e. [HNO_3] = 8.5M at 95°C, stirring rate of 300 rpm), in order to look at the specific effect of the Pu content on dissolution of $(U_{1-x}Pu_x)O_{2\pm\delta}$. The determination of the concentration of plutonium in solution allows calculation of the mass of dissolved oxide and thus the percentage of powder dissolved at each instant. All these percentages lead to a linear relationship between dissolution kinetic rate of oxide and Pu content. The dissolutions of oxides of different Pu content are illustrated in Figure 5. As it has already been reported in the scientific literature, increasing the Pu content leads to a decrease in kinetics. A factor close to one thousand is observed between the dissolution kinetics of $U_{0.64}Pu_{0.36}O_{2\pm\delta}$ and PuO_2. However here, the dissolution rate of the PuO_2 appears faster than the dissolution rate of the $U_{0.24}Pu_{0.76}O_{2\pm\delta}$, the phenomenon can be explained by morphological parameters making the PuO_2 powder more favorable to dissolution than the $U_{0.24}Pu_{0.76}O_{2\pm\delta}$ (due to lower crystallite size and higher specific surface area of the PuO_2 powder). The dissolution kinetics rate of the $U_{0.64}Pu_{0.36}O_{2\pm\delta}$ powder is obtained only from two experimental points, because of a high reactivity of this powder. Table 1 presents similar morphological parameters for the studied compounds, with only a factor of 4 between the smallest and largest crystallites size and a factor of 15 between the lowest and highest specific surface area. Hence, there is a consequent effect of the Pu content on the dissolution kinetics. Some tests were carried out under similar experimental conditions on powders with lower Pu content (25% and less) but dissolution rates were too fast to be experimentally measured.

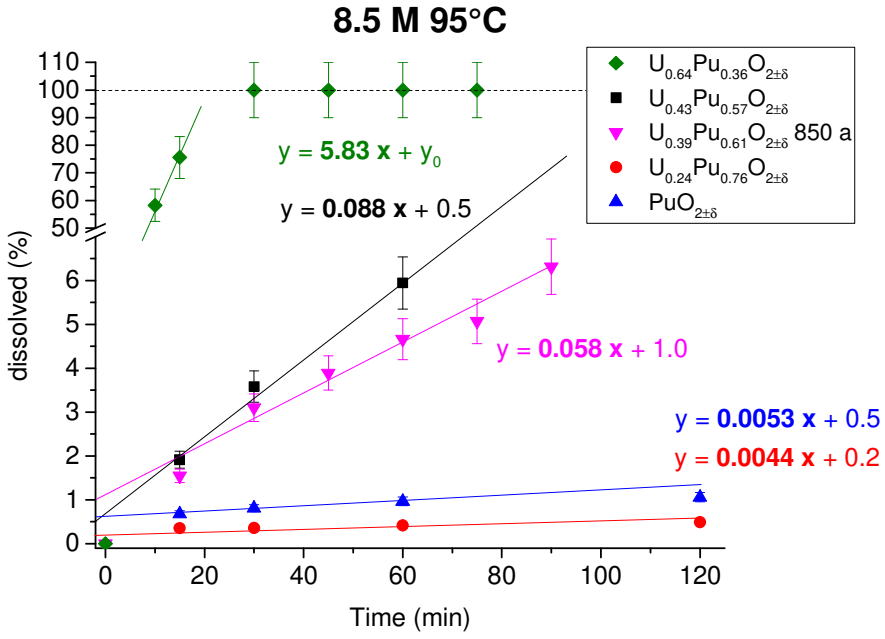

Figure 5 : Dissolution of $(U_{1-x}Pu_x)O_{2\pm\delta}$ powders with different Pu contents and different morphologies in the same experimental conditions ([HNO_3]=8.5mol.L^{-1} at 95°C).

It is then possible to quantify the effect of the Pu content of the oxide on its dissolution kinetics rate in nitric acid of 8.5M concentration at 95°C using the determined k value for the different Pu contents studied from Figure 5. The different k values are summarized in Table 2, column "experiment k". By plotting the logarithmic functions of the constant k according to the Pu content, a line is obtained (Figure 6) defining by the regression presented in equation 3.3.1, k value for the Pu content of 57% was not taken into account for this linear regression in order to be used as a validation point. This empiric law defines an effect of Pu content on dissolution kinetics following an exponential function for a range of Pu content between 36 and 100%. The phenomenon is similar to the findings of Ikeuchi [3] in the range of 18 to 29% Pu.

Table 2 : k values for dissolution of $(U_{1-x}Pu_x)O_{2\pm\delta}$ with varying Pu content, in nitric acid 8.5M at 95°C.

%Pu	Log %Pu	experiment k	Log k
36	1.56	374	2.57
61	1.79	0.19	-0.72
		2.53	0.40
		2.60	0.41
76	1.88	1.58	0.20
100	2.00	0.05	-1.30
57	1.76	7.04	0.85

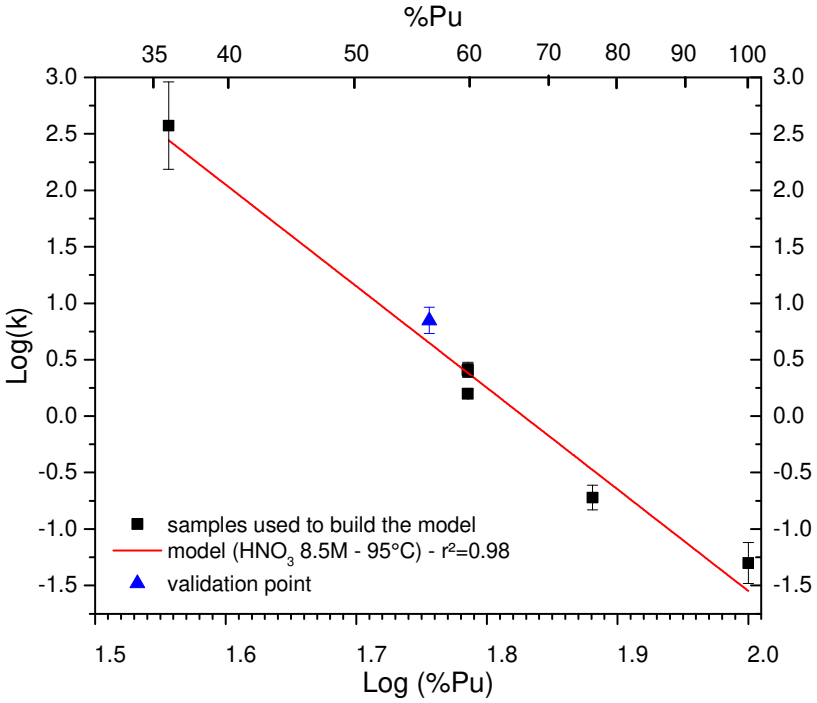

Figure 6: Relation between the kinetic rate constant and the Pu content of the oxide at 8.5 mol.L^{-1} heated at 95°C.

$$k = \%Pu^{-9.0} * 10^{-16.4} \qquad 3.3.1$$

With %Pu the plutonium content of the oxide powder in percent and k in nm^{-1}.m$^{-2/3}$.g$^{1/3}$.%dissolved^{1}.min^{-1}.

It may to be noticed that between the two limits of the tested interval (36% and 100% of Pu) the dissolution kinetics rate is multiplied by almost 7500. Looking at the validation point, the model k value for 57% of Pu, is 4.44 for an experiment value of 7.04, so a difference of only 37%. Considering k evolution with respect to Pu content, such little difference between model and experiment figures is acceptable as a slight uncertainty in Pu content could explain this result: a Pu content of 58% rather than 57% would induce a variation of k by 57% for example. Therefore, it is possible to conclude that the effect of the Pu content on the dissolution kinetics can be defined by a power function. As mentioned, the parameters of the function are valid for dissolution in nitric acid of 8.5M concentration at 95°C only. The future work of such study could be to look at the effect of acidity and temperature on the different parameters of the laws used, in order to define a general law modelling the dissolution of $(U_{1-x}Pu_x)O_{2\pm\delta}$ irrespective of the morphologic properties of the powder, its composition (Pu content) and the dissolution conditions (acidity and temperature).

4. Conclusion

The characterization tools employed in this study were used to describe the Pu content and the morphology of the different powders. As the calcination temperature increases the crystallite size increases resulting in decrease in specific surface area, which is in agreement with literature data.

For the different morphologies of same oxide $U_{0.39}Pu_{0.61}O_{2\pm\delta}$, a kinetic law has been validated to describe the effect induced by the morphology on the dissolution rates. Although the physical relationship between the dissolution rates and the described morphological properties has not yet been described, mathematically there seems to be a close link between specific surface area, crystallite sizes and the dissolution kinetics of the oxide powders.

Present study indicates a decrease in dissolution kinetics with the increase in Pu content of (U,Pu) oxide. Despite a difference of a factor of about 7500 between the dissolution kinetics of $U_{0,64}Pu_{0,36}O_{2\pm\delta}$ and PuO_2, an empirical law could be established and validated describing the effect of the Pu content on dissolution rates at 8.5 mol.L^{-1} HNO_3 concentration at 95°C.

Acknowledgements

This research was partly funded by ORANO, France. The authors specially thank C. Lavalette (ORANO) for encouraging this PhD work and for fruitful discussions. Another part was funded under the framework of the European H2020 GENIORS Project (Contract n: 730227).

References

[1] A.L.Uriarte, R.H.Rainey, *Dissolution of high-density UO2, PuO2, and UO2-PuO2 pellets in inorganic acids*, ORNL-3695, 1965.

[2] R.E.Lerch, *Dissolution of unirradiated mechanically blended, sol gel, and coprecipitated mixed oxide fuel*, HEDL-TME 72-67, 1972.

[3] H. Ikeuchi, A. Shibata, Y. Sano, T. Koizumi, *Dissolution of irradiated mixed-oxide fuels with different plutonium contents,* Procedia Chemistry 7 , 77-83, 2012.

[4] D.Vollath, H.Wedemeyer, *On the dissolution of (U,Pu)O_2 solid solutions with different Pu contents in boiling nitric acid*, Nuclear technology 71, 1985.

[5] Y.Ziouane, B.Arab-Chapelet, S.Lalleman, G.Leturcq, *Effect of the microstructural morphology on UO_2 powders*, Procedia Chemistry 21, 319-325, 2016.

[6] D.E.Horner, D.J.Crouse, J.C.Mailen, *Cerium promoted dissolution of PuO_2 and PuO_2-UO_2 in nitric acid,* ORNL/TM-4716, 1977.

[7] G.F.Molen, *Dissolution of Plutonium Oxide,* RFP-922, UC-4 Chemistry, TID-4500, 1967.

[8] Y.Ziouane, T. Milhau, M. Maubert, B. Arab-Chapelet, G. Leturcq, *Dissolution kinetics of CeO2 powders with different morphologies and analogy to PuO2 dissolution*, Hydrometallurgy 177, 205-213, 2018.

[9] http://www.chemguide.co.uk/physical/phaseeqia/nonideal.html

[10] Vaidya V.N *Sol-gel process for ceramic nuclear fuels*. Journal of Sol-Gel Science and Technology, 369-381, 2008.

[11] Jeong K-C, Kim Y-K, Oh S-C, Cho M-S, Lee Y-W, Chang J-W. *UO3 intermediate particle preparation using the Sol-gel process*. Transactions of the Korean Nuclear Society autumn meeting Busan, Korea, October 27-28, 2005.

[12] Robisson A-C, Lemonnier S, Grandjean S, *Sol-gel chemistry applied to the synthesis of actinide-based compounds for the fabrication of advanced fuels*, ATALANTE 2004.

[13] X.Machuron-Mandard, *Étude de la cinétique et du mécanisme de la réaction de dissolution du bioxyde de plutonium par l'ion Cr (II) en solution acide*, PhD thesis from University of Paris VI, 1991.

[14] L.Claparede, F.Tocino, S.Szenknect, A.Mesbah, N.Clavier, P.Moisy, N.Dacheux, *Dissolution of $Th_{1-x}U_xO_2$: Effects of chemical composition and microstructure*, Journal of Nuclear Materials, Volume 457, 304-316, 2015.

[15] DIFFRACplus TOPAS/TOPAS R/TOPAS P Version 2.1 and www.bruker-axs.com.

[16] Cheary R.W, Coelho A.A, Cline J.P., *Fundamental parameters line profile fitting in laboratory diffractometers. J. Res. Natl. Inst. Stand. Technol*. 109, 1-25, 2004.

[17] Fagerlund G., *Determination of specific surface by the BET method*. Materials and structures volume 6: 239-245 , 1973.

[18] C. Maillard, G. Pédehontaa-Hiaa, E. Esbelin, C. Rivier, D. Roudil. *Optimization of U and Pu traces separation by chromatography for analytical purposes : influence of U/Pu mass ratio,* Journal of Radioanalytical and Nuclear chemistry317: 1253-1261, 2018

[19] W.J. Young, L. Lynds. *An X-Ray and density study of nonstoichiometry in uranium oxides*. Atomic International (USA) report, NAA-SR-6765, 1962.

[20] A.J. Freeman, J.B. Darby Jr, *The actinides – Electronic structure and related properties*, Vol II, Material Science Series, ISBN 0-12-266702-6, 1974.

[21] B. Arab-Chapelet, F. De Bruycker, S. Picart, G. Leturcq, S. Grandjean, *Structural characterization of mixed uranium-plutonium co-precipitates and oxides synthesized by oxalic co-conversion route*, ATALANTE 2008, Montpellier, 19-22 May 2008.

[22] Y.B. Rao, R.B. Yadav, R.N. Swamy, B. Gopalan, S. Syamsundar, *Determination of specific surface area of uranium oxide powders using differential thermal analysis technique*, Journal of thermal analysis vol 44, pages 1439-1448, 1995.